Polymers suppress the inverse transfers of energy and the enstrophy flux fluctuations in two-dimensional turbulence

H. Kellay
CPMOH, Université de Bordeaux I, 351 Cours de la Libération, 33405 Talence, France
(Received 2 August 2003; revised manuscript received 26 April 2004; published 20 September 2004)

The addition of minute amounts of a flexible polymer to two-dimensional turbulence produced in fast-flowing soap films affects large scales and small scales differently. For large scales, the inverse transfers of energy are suppressed. For small scales, where mean quantities are barely affected, the enstrophy flux fluctuations are significantly reduced, making the flow less chaotic.

DOI: 10.1103/PhysRevE.70.036310 PACS number(s): 47.27.Gs, 83.50.−v

I. INTRODUCTION

The effects of polymers, even at very low concentrations, on flows at both low and high Reynolds numbers can be significant [1]. Such effects can be used for practical purposes such as mixing or reduction of drag and for fundamental reasons such as the interaction of flow, a turbulent flow, say, with the different degrees of freedom of such complex molecules. At rest, these molecules are coiled up into very small balls, while under flow, they may stretch considerably. This interaction may end up giving clues to the problem of turbulence itself. Recent experiments, simulations, and theory in two dimensions are bringing in new information as to how this interaction works and what its consequences are [2–5]. The two-dimensional situation is simple relative to its three-dimensional counterpart, mainly due to the absence of vortex stretching. These calculations focus on the elongation of the polymer molecules and make definite predictions about the statistics of the polymer elongation and its reaction on the flow field.

Polymers affect decaying two-dimensional turbulence in a surprising way, as we have demonstrated recently [2]. Their presence seems to affect the large scales in a significant way: their amplitude in the energy density spectrum can be reduced by an order of magnitude upon addition of minute amounts of polymer. The small scales, however, were hardly affected. In contrast, for three-dimensional turbulence, the results seem to indicate suppression of fluctuations at all scales [1]. However, the role of the boundaries complicates the analysis as most of the stretching may occur in the boundary layer [6].

We carry out a more detailed study here to further explore the role of the polymers on two-dimensional turbulence. Notably, by measuring both the velocity and the vorticity in a two-dimensional turbulent flow, we find that the polymers affect both the large scales and the small scales. The presence of the polymers inhibits the inverse transfers of energy, which are measured directly here, thereby reducing large-scale fluctuations of the velocity and the vorticity. A more subtle effect is evidenced at the small scales where the fluctuations of the enstrophy flux are significantly reduced. The reduction of these fluctuations is in line with recent simulations showing that the distribution of the Lyapunov exponents of the flow is much narrower in the presence of the polymer reducing the chaoticity of the flow, in agreement with these simulations [3].

II. BRIEF SUMMARY OF EXPERIMENTAL RESULTS ON TURBULENT SOAP FILMS

The experiments use rapidly flowing soap films, where the turbulence is generated using a horizontal array of equally spaced cylinders or a combination of horizontal and vertical grids. The properties of turbulence in such films (for the horizontal array of cylinders) have been studied at length and show the presence of an enstrophy cascade and the growth of the integral scale as expected for decaying two-dimensional turbulence [7]. When vertical and horizontal grids are used, two ranges coexist: the first one at large scales shows an inverse energy cascade with a $-5/3$ scaling exponent for the energy density, and the second one at smaller scales shows an enstrophy cascade with a -3 scaling exponent [7–9]. There have been few measurements so far of the vorticity statistics in these flows [7]. For horizontal grids, the results of Kellay *et al.* [10] indicated that the enstrophy spectrum scales as $e(k) \sim k^{-2}$. Rivera *et al.* [11] found an exponent of 0.4 for the second moment of vorticity increments versus the increment r for the same case. Theoretically, the enstrophy scaling exponent is -1 (with logarithmic corrections) while the second moment of vorticity increments should display, according to recent theory, logarithmic corrections [12]. The absolute value of the enstrophy flux, however, was found to scale roughly linearly versus the increment r by Kellay *et al.* [13] and Rivera *et al.* [11] as expected, but the sign of the enstrophy flux was not determined. The probability density functions (PDFs) of this flux showed stretched exponential forms [13]. Direct numerical simulations of a similar flow situation to the above-cited experiments reproduced most of the features found in the experiments of Kellay and co-workers [13,14]. Clearly, the properties of the vorticity statistics in this decaying two-dimensional turbulence deviate from expectations. Similar results for the vorticity spectrum were also found by Bruneau and Kellay [9] for the case where the two cascades coexist.

Measurements of the thickness fluctuations, on the other hand, produced a surprise for the case of decaying turbulence (horizontal grid alone), as shown by Greffier *et al.* [15]. In-

deed, the power spectrum of the thickness fluctuations scales versus the wave number with an exponent of $-5/3$ as in the inverse cascade range, despite the fact that the velocity fluctuations present a scaling consistent with the presence of an enstrophy cascade. The addition of polymers changed the thickness fluctuations drastically [2] and the exponent for the scaling of the thickness power spectrum turned out to be close to -1, as expected for an enstrophy cascade range and therefore consistent with the scaling of the velocity fluctuations. Since the polymer significantly reduced the third moment of velocity differences (which is positive without the polymer, indicating the presence of an inverse transfer of energy [7]), it was conjectured [2] that the polymer inhibits vortex merging, which is responsible for the transfer of energy upscale.

III. EXPERIMENTAL TECHNIQUES AND RESULTS

The soap films used are vertical with a length of 2 m and a width of 5 cm. The soap water (1% detergent in water) was pumped with a small micropump to the top of the channel (with a V-shaped entrance) made of nylon wires. The velocities reached in such a channel hover at around 2 m/s with turbulent intensities that can be as high as 15%. The Reynolds numbers reached are of order 10 000. A schematic of the experimental setup is shown in Fig. 1. When the polymer was used, the pump was not used and the soap water was brought to the top of the channel from a reservoir placed higher up. The grids used are either horizontal arrays of cylinders or a combination of horizontal and vertical grids (U-shaped grid). The horizontal grid was composed of seven equally spaced (7 mm spacing) cylinders 3.5 mm in diameter [see Fig. 1(a)]. The U-shaped grid had five equally spaced cylinders (spacing 1 cm) 5 mm in diameter for the horizontal array and two vertical arrays placed on the side of the channel with ten cylinders each (spacing 1 cm) of diameter 2 mm. A schematic of this configuration is shown in Fig. 1(b). Unlike the horizontal grid alone, this configuration allows for the injection of the vorticity from the sides of the channel, as shown in the photograph of Fig. 1(c). Here one clearly sees intense activity due to the presence of the small side cylinders. This injection of the vorticity from the sides allows for the establishment of both an inverse energy cascade and a regime that is consistent with an enstrophy cascade, as shown recently by Bruneau and Kellay [9]. Such a geometry was explored a few years ago by Rutgers [8], who argued that the turbulence produced this way is close to a forced turbulence situation.

The velocity fluctuations are measured using laser Doppler velocimetry. To measure the vorticity statistics, we use two laser Doppler velocimeters. This technique (the use of two velocimeters to measure vorticity fluctuations) has been described in detail elsewhere [7,10] and permits us to record a time trace of the velocity and the vorticity in a single point. Since time traces of the velocity or vorticity are taken at a fixed point in the flow, the Taylor frozen turbulence assumption is used to convert time to length scale: $l=V/f$, where V is the mean flow velocity and f is the frequency. Results from previous experimental determinations of the vorticity

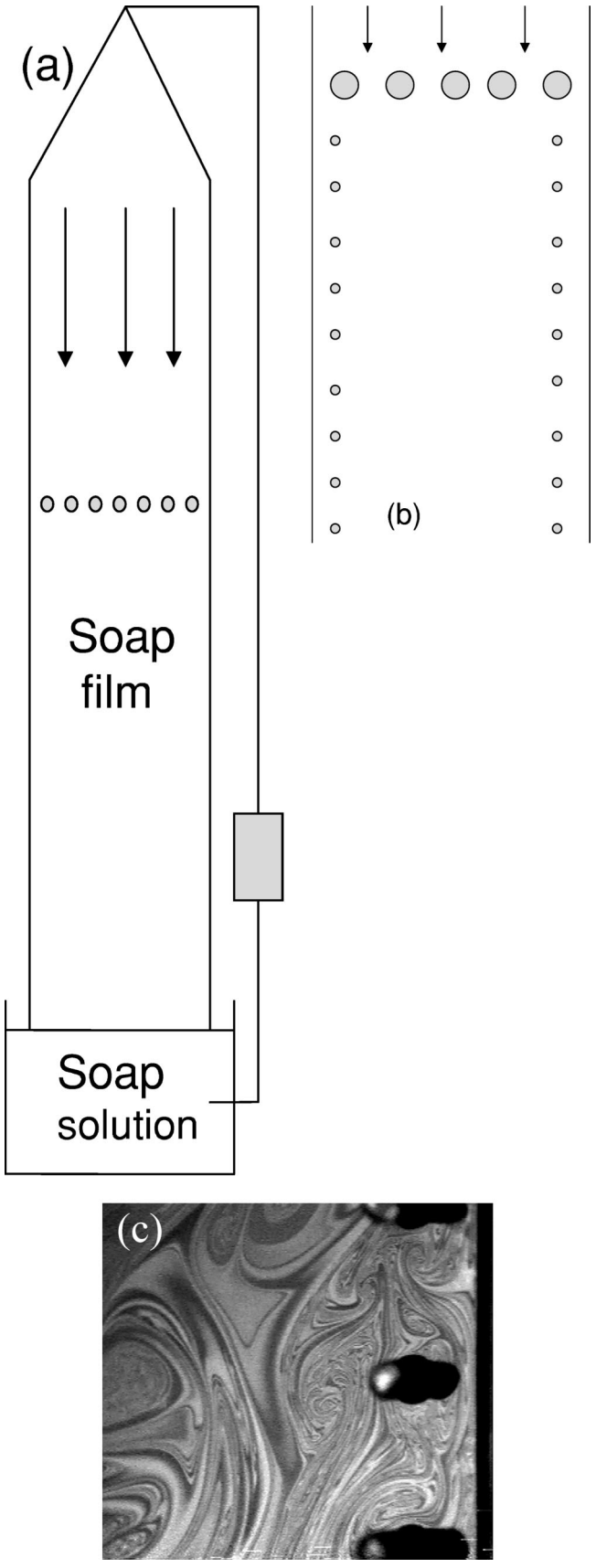

FIG. 1. (a) Schematic of the soap film channel. (b) The U-shaped grid configuration.

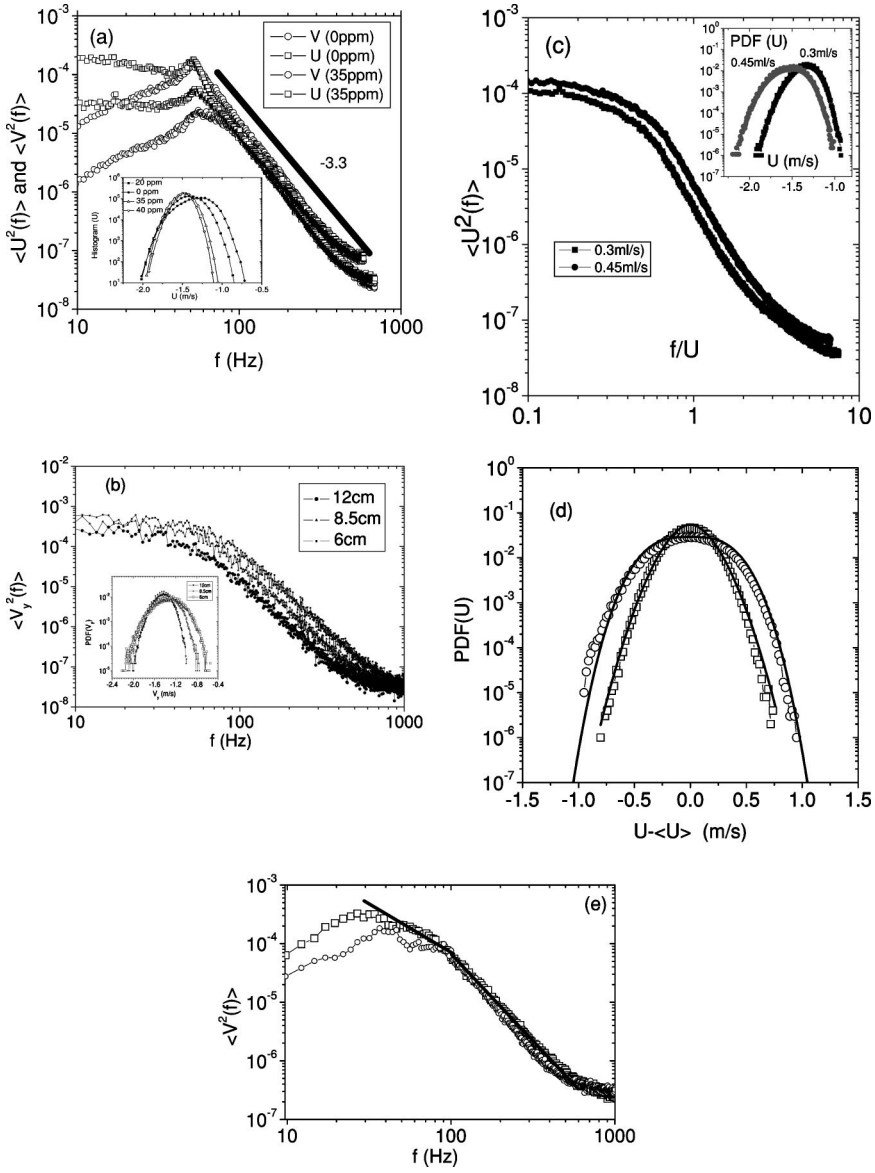

FIG. 2. Power spectra of the velocity fluctuations. (a) At a distance of 8 cm from the horizontal grid and different polymer concentrations [polyethyleneoxide (PEO) (molecular weight 4M), in parts per million (ppm) by weight]; inset: histograms of the longitudinal velocity U. (b) Velocity power spectra obtained at different distances from the grid: The turbulence intensity decreases as the distance is increased, as shown in the inset. (c) Velocity power spectra obtained for two different flux: The turbulence intensity decreases as the flux is decreased, as shown in the inset. (d) Probability density functions of the velocity fluctuations with and without polymer. The solid lines are fits as indicated in the text. (e) Velocity power spectra at a distance of 22 cm from the U-shaped grid with a horizontal and two vertical arrays of cylinders (squares: 0 ppm, circles: 20 ppm).

using this technique have been found in excellent agreement with direct numerical simulations of grid turbulence (a geometry very similar to the one used here) [9,10,13,14].

The polymer used is polyethyleneoxide (PEO) with a molecular weight of 4×10^6. At equilibrium, the polymer is in a coiled state with a well-defined radius of gyration. If perturbed, the coil relaxes with a well-defined relaxation time. This so-called Zimm relaxation time ($\tau\sim\eta R_g^3/k_BT$, where η is the solvent viscosity, R_g is the radius of gyration, k_B is the Boltzmann constant, and T is the temperature) for this polymer is of order 1 ms as determined from measurements of the radius of gyration of the polymer in water. While a few tests were carried out using a higher molecular weight, the reproducibility of the results was much better with the smaller molecular weight. Degradation and breaking of the polymer is the main problem with the high molecular weight. Note that at the small concentration used here, the viscosity of the soap solution is hardly affected.

A. Velocity fluctuations and energy transfers

Let us first recall the major results already obtained in our previous work [2] on the effects of polymers on two-dimensional turbulence. Figure 2(a) shows the velocity power spectra, which, in agreement with our previous results, show a large reduction in amplitude at large scales when the horizontal grid is used alone. The probability density functions (PDFs) of the velocity are also narrower with the polymer, as seen in the inset. The measurements are taken at 8 cm from the horizontal grid [seven equally spaced (7 mm) cylinders 3.5 mm in diameter] where the mean velocity was 1.8 m/s and the turbulence intensity was 10%. For a range of scales between 2 mm and 2 cm, the turbulence is isotropic with a clear scaling seen for both components of the velocity. The exponent for both the polymer solution and the polymer-free solution is about −3.3, close to (but slightly higher than) the predicted exponent for the enstrophy cascade range, which is −3. Logarithmic corrections

to this scaling law are expected theoretically. The velocity spectra show a reduction in the amplitude of the large scales and little effects at small scales when the polymer is used. This effect can be compared to results obtained without a polymer but for realizations with different turbulent intensities, as shown in Fig. 2(b). Indeed, when measurements are taken at different locations, the mean velocity increases as the distance to the grid increases, while the turbulent intensity decreases. This is shown in the inset to Fig. 2(b). While the PDFs of the velocity versus distance from the grid show similar trends to the effect of the polymer, the spectra of the velocity show a different behavior. As can be seen in Fig. 2(b), the spectral density decreases at all frequencies for a simple decrease of the turbulent intensity obtained at different locations from the grid. For the polymer, only the large scales are affected and suppressed while the small scales remain intact. This goes to show that the polymer effect is nontrivial and not simply related to the injection of less energy into the system. Similar results are also obtained by changing the flux at a fixed location. The reduction of the flux also reduces the turbulent intensity, but the reduction for the spectra is seen at all frequencies, as seen in Fig. 2(c). Again, the reduction of the injected energy is not sufficient to explain the polymer effect. As mentioned in the Introduction, the nontrivial effect of the polymer can be captured in numerical simulations where the polymer effect is taken into account through additional stresses in the Navier-Stokes equations. Another consequence of the polymers is to change the functional shape of the probability density functions of the velocity, as seen in Fig. 2(d). The PDFs change from super-Gaussian to sub-Gaussian, as indicated by the solid lines, which are fits to the data using the following functional forms: $\exp(-c_1|u|^3)$ and $\exp(-c_2|u|^{1.8})$, where c_1 and c_2 are two positive constants. These two functional shapes are in excellent agreement with the results of Celani *et al.* [3] and Benzi *et al.* [5].

While the above-mentioned measurements are obtained in the case of an enstrophy cascade alone, here we also evidence this effect in the case where the two cascades coexist. To obtain this situation, we used a U-shaped grid with five cylinders (diameter 5 mm spaced by 1 cm) placed horizontally and two series of vertical grids (ten cylinders of diameter 2 mm and a spacing of 1 cm) on each side of the channel. This is similar in spirit to the grids introduced by Rutgers [8] to obtain the coexistence of the two cascades. Figure 2(e) shows a similar phenomenon in the case where horizontal and vertical grids are used. In this case, a $-5/3$ range at large scales for the energy density is clearly seen without the polymer. The presence of the polymer destroys this scaling and reduces the amplitude of the spectrum at large scales, an effect also seen in numerical simulations [16]. The small scales, however, seem to show no change and the -3 scaling range stays intact. For both types of grid, the reduction of the large-scale velocity fluctuations is clearly seen, indicating that the inverse transfers of energy from small to large scales are inhibited by the presence of the polymer.

A more direct test of this is a direct measurement of the spectral transfer function $T(k)$ whose origin is the nonlinear term in the Navier-Stokes equations [$\partial E(k)/\partial t = T(k) + \nu k^2 E(k)$, where ν is the kinematic viscosity and $E(k)$ is the energy density function]. An expression for this in two dimensions has been calculated by Van Atta [17] and makes use of the following triple correlation functions: $S_{111}(r) = \langle u^2(y)u(y+r)\rangle$ and $S_{212}(r) = \langle v(y)u(y)v(y+r)\rangle$. Here u is the longitudinal velocity, v is the transverse velocity, and r is a spatial increment in the direction of the flow (parallel to u). These correlations have been evaluated directly from the velocity signals at one point (the Taylor hypothesis being invoked). The expression for the transfer function reads $T(k) = -2k/\pi^2 \int_k^\infty \int_0^\infty r S_{i1i}(r)\cos(k_1 r)\, dr[k_1 dk_1/\sqrt{(k_1^2 - k^2)}]$ $(i=1,2)$. Figure 3 displays the $T(K)$ obtained without polymer and with a small polymer concentration for the horizontal grid. One of the main features of these $T(k)$ is the presence of two bumps: a negative bump at large k and a positive one at small k. This is the hallmark of two-dimensional turbulence showing a transfer of energy from small to large scales. The presence of the polymer affects both bumps whose amplitudes are reduced. For the polymer solution, both bumps shrink in extent and shift slightly to higher wave numbers for the positive bump and to lower wave numbers for the negative one. Basically, the polymer reduces the transfer of energy upscale, thereby reducing the large-scale fluctuations. Similar results were obtained for the case where the two cascades coexist.

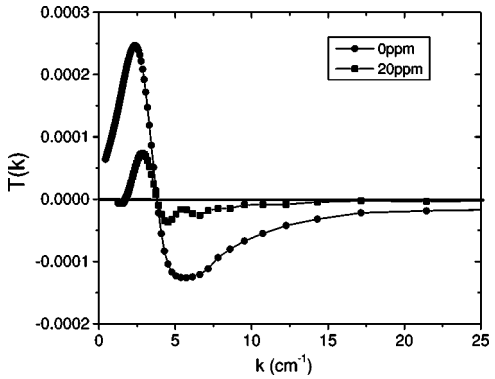

FIG. 3. Transfer function $T(k)$.

B. Vorticity fluctuations and enstrophy flux

In our previous study, no information was obtained on the vorticity fluctuations. Here we present a study of the statistics of the vorticity and the enstrophy flux. In Figs. 4(a) and 4(b), we show the vorticity power spectrum for the bare soap film and for a 25 ppm PEO solution (the PEO was mixed with the soap solution, which consists of 1% commercial detergent in water; the molecular weight of the polymer was 4 000 000). The vorticity power spectra show a trend similar to the velocity spectra with a large reduction at large scales for both the horizontal grid and the combination of horizontal and vertical grids. In the absence of the polymer, the vorticity power spectrum shows an exponent close to -2, in agreement with previous experiments and numerical simulations. In the presence of the polymer, the scaling exponent does not change and comes out to be -2 as well but for a smaller range. The second-order vorticity structure function

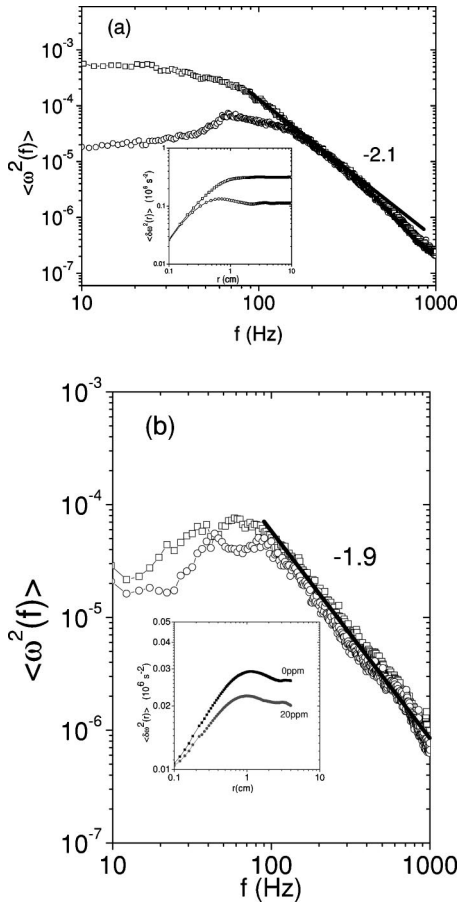

FIG. 4. Power spectra of vorticity fluctuations. (a) Horizontal grid (squares: 0 ppm, circles: 25 ppm); inset: second-order vorticity structure function. (b) Horizontal and vertical grid (squares: 0 ppm, circles: 20 ppm); inset: second-order vorticity structure function.

$\langle \delta\omega^2(r) \rangle$ also shows a reduction in amplitude for large scales in the presence of the polymers, as shown in the insets to Fig. 4. The PDFs of the vorticity increments were also measured for the two different grids. In both situations (with and without the polymer), the PDFs have exponential tails at small enough scales, indicating large deviations from the mean. The PDFs without the polymer for the horizontal grid alone become Gaussian at relatively smaller scales than the case of horizontal and vertical grids. We noticed that the width of the PDFs changes more rapidly in the absence of the polymer, which is consistent with the measurements of the second-order structure function. The polymer seems to give way to a large range where the vorticity structure function is roughly constant. Theory predicts that this structure function should be flat within logarithmic corrections. The variation of the PDFs with r for the polymer case seems to be consistent with this prediction.

Another way to examine the effects of the polymer on the flow field is to study the enstrophy flux $F = \delta u(r)\,\delta w^2(r)$. For both types of grid, the first moment of F starts out roughly linearly versus the increment r, as seen in Figs. 5(a) and 5(b), before going through a maximum and decreases to zero at larger r. It is only at very small scales that this flux is negative. The position of the maximum shifts to smaller scales

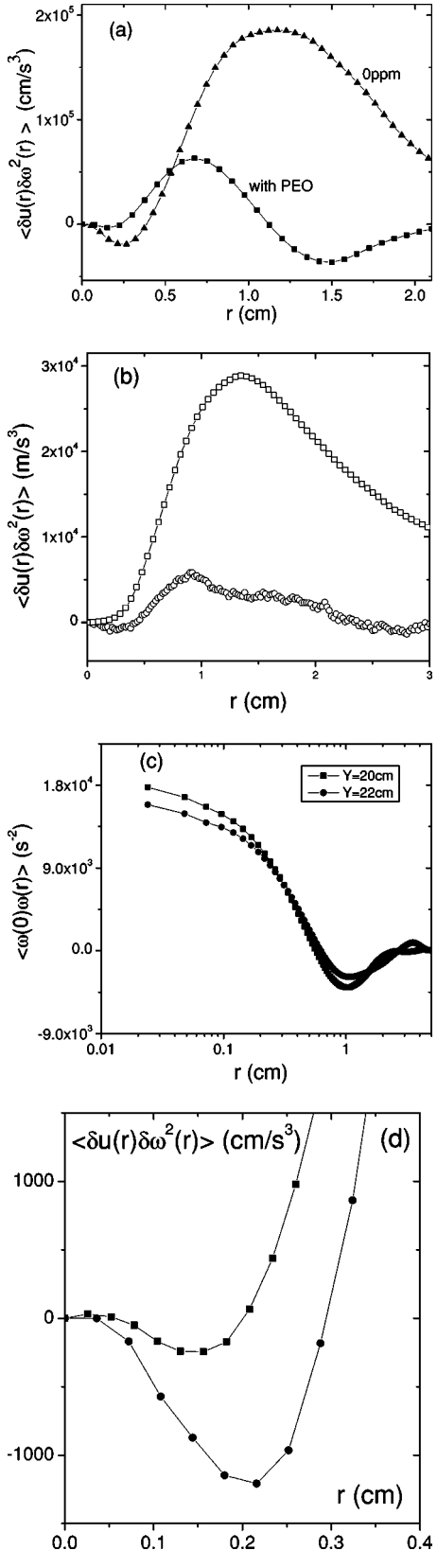

FIG. 5. First moment of the enstrophy flux F vs the increment r: (a) horizontal grid, (b) horizontal and vertical grids, (c) vorticity correlation function at two different distances from the U-shaped grid, (d) a closeup of the small-scale region for the enstrophy flux for the U-shaped grid.

when the polymer is used while the amplitude of the maximum gets reduced. On the basis of one of the few exact results on the enstrophy cascade, this moment is supposedly negative, which is true only at very small scales in our case and not for the full range where the −3 scaling exponent is observed. One possibility is that the rate of change of the vorticity correlation function with distance from the grid plays a role. One can actually write the first moment of F and its relation to the rate of change of the vorticity correlation function for decaying 2D turbulence, as has been suggested recently [9], which gives a qualitative explanation for the shape of the enstrophy flux versus the increment r. Indeed this calculation gives $\langle F\rangle = 2\int_0^r d/dt\langle\omega(0)\omega(r)\rangle dr$. [This expression reduces to the known result $\langle F\rangle = -2\beta r$ if one keeps just the single point rate of change of the enstrophy $(d/dt\langle\omega^2\rangle = -\beta)$.] Since the vorticity correlation functions, taken at different locations and therefore for different times of evolution, present a decrease at small scales and an increase at larger scales as time increases [see Fig. 5(c)], the time derivative of the correlation function changes sign from negative to positive as r increases, just like the measured $\langle F\rangle$. Figure 5(a) shows a negative part for the horizontal grid at small scales. Figure 5(d) shows a closeup of the very-small-scale region where the enstrophy flux is negative for two different realizations for the U-shaped grid without the polymer; the negative part with the polymer is visible in Fig. 5(b). The crossover from negative to positive flux occurs at roughly 2–3 mm, just like the crossover observed for the vorticity correlation functions. This explanation is similar to the one proposed by Belmonte *et al.* [7] for the measurements of the third moment of velocity differences in these turbulent soap films. For these latter measurements, the rate of change of the velocity correlation function with distance from the grid (which shows a trend similar to the vorticity correlation functions versus this distance) was responsible for the positivity of this third moment. Clearly, the decay of the turbulence, and therefore the inhomogeneity of the flow in the longitudinal direction, plays a major role in determining the sign of the enstrophy flux.

Very recent experiments [18] show that the enstrophy cascade is only weakly forward (i.e., from large to small scales) with considerable "backscatter"; only at very small scales (comparable to the range where our measurements also show a negative flux) did this flux become negative. Our results seem to be in line with these measurements carried out using a different technique, namely particle image velocimetry. Apart from these considerations, the polymer reduces the amplitude of the enstrophy flux at large scales.

A more notable effect of the addition of the polymer is a large reduction of the fluctuations of the enstrophy transfer rate at small scales. The PDFs of F are double-sided stretched exponentials for both cases, as seen in Fig. 6(a) and 6(b) for different values of the increment r in the enstrophy cascade range. This is in agreement with previous measurements and numerical simulations [13]. Our main result is that the PDFs of $F/r = \delta u(r)\delta w^2(r)/r$ (proportional to the enstrophy flux β) have a much narrower width with the polymer for the decaying turbulence [horizontal grid, Fig. 6(a)]. The inhibition of the enstrophy flux fluctuations is in line

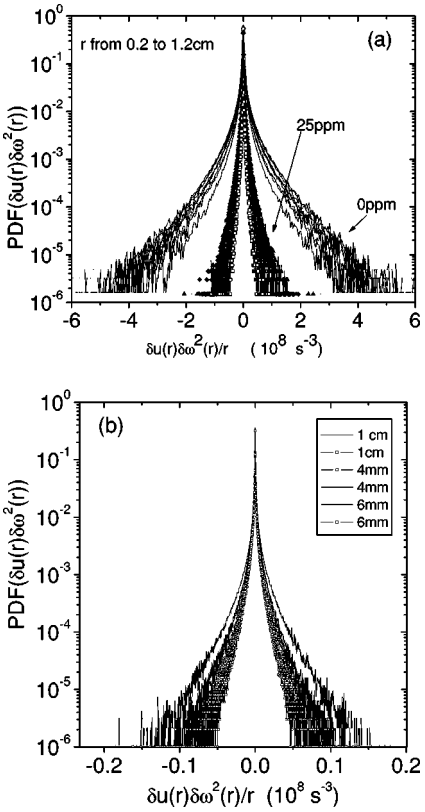

FIG. 6. Probability density functions of F/r for different values of r: (a) horizontal grid, (b) horizontal and vertical grids.

with recent simulations of the effects of polymers on 2D turbulence. These simulations found a reduction in the fluctuations of the Lyapunov exponents of the flow [3]. These exponents can be identified with the rate of enstrophy transfer β. This reduction gives way to a less chaotic flow. For the case where the two cascades coexist, the fluctuations of F/r are much less violent [Fig. 6(b)]. Here the polymer shows a very small reduction of these fluctuations. In fact, the effect of the polymer is more important when the strain rates (the distribution of F/r is a measure of the distribution of strain rates) are comparable to the relaxation time of the polymer. The polymer used here (PEO, molecular weight of 4 000 000) has an inverse of the Zimm relaxation time close to 1000 Hz. The values $\beta^{-1/3}$ observed for the decaying case can be as large as 800 Hz. When the polymer is used, the largest values observed are rather close to 400 Hz [Fig. 6(a)]. In the case where the two cascades coexist [Fig. 6(b)], the largest values do not exceed 200 Hz. That the polymer affects flows with strains comparable to the inverse relaxation time of the polymer has been anticipated theoretically [4,3], seen in simulations [3], and evidenced in experiments on detaching drops of polymer solutions [19]. Our findings are in agreement with these observations.

IV. CONCLUSION

In conclusion, polymers affect two-dimensional turbulence both at large scales and at small scales. At large scales, the reduction of the inverse transfers of energy leads to a

reduction of the velocity and the vorticity fluctuations at these scales. The reduction of the enstrophy flux fluctuations operates at small scales when the strain rates present are comparable to the inverse relaxation time of the polymer. We believe that our results, in combination with the theoretical work mentioned above, bring the subject of drag reduction, a long-standing issue, within reach for two-dimensional turbulence.

[1] B. A. Toms, in *Proceedings of the International Congress on Rheology* (North Holland, Amsterdam, 1949); J. L. Lumley, J. Polym. Sci., Part D: Macromol. Rev. **7**, 263 (1973); A. Gyr and H. W. Bewersdorff, *Drag Reduction of Turbulent Flow by Additives* (Kluwer, Dordrecht, 1995); K. R. Sreenivasan and C. M. White, J. Fluid Mech. **409**, 149 (2000).

[2] Y. Amarouchene and H. Kellay, Phys. Rev. Lett. **89**, 104502 (2002).

[3] G. Boffetta, A. Celani, and S. Musacchio, Phys. Rev. Lett. **91**, 034501 (2003).

[4] E. Balkovsky, A. Fouxon, and V. Lebedev, Phys. Rev. Lett. **84**, 4765 (2000); M. Chertkov, *ibid.* **84**, 4761 (2000).

[5] R. Benzi, N. Horesh, and I. Procaccia (unpublished).

[6] O. Cadot, D. Bonn, and S. Douady, Phys. Fluids **47**, 10 (1998).

[7] H. Kellay and W. I. Goldburg, Rep. Prog. Phys. **69**, 845 (2002).

[8] M. Rutgers, Phys. Rev. Lett. **81**, 2244 (1998).

[9] C. H. Bruneau and H. Kellay (unpublished).

[10] H. Kellay, X. L. Wu, and W. I. Goldburg, Phys. Rev. Lett. **80**, 277 (1998).

[11] M. Rivera, P. Vorobieff, and R. E. Ecke, Phys. Rev. Lett. **81**, 1417 (1998).

[12] G. Falkovich and V. Lebedev, Phys. Rev. E **49**, R1800 (1994).

[13] H. Kellay, C. H. Bruneau, and X. L. Wu, Phys. Rev. Lett. **84**, 1696 (2000).

[14] C. H. Bruneau, O. Greffier, and H. Kellay, Phys. Rev. E **60**, R1162 (1999).

[15] O. Greffier, Y. Amarouchene, and H. Kellay, Phys. Rev. Lett. **88**, 194101 (2002).

[16] A. Celani (private communication).

[17] C. Van Atta (private communication).This expression was obtained by Van Atta and communicated to us (W. I. Goldburg and myself) in 1994. Its derivation follows the same reasoning [see also G. K. Batchelor, *The Theory of Homogeneous Turbulence* (Cambridge University Press, Cambridge, UK, 1953)] as in C. W. Van Atta and W. Y. Chen, J. Fluid Mech. **38**, 743 (1969).

[18] M. K. Rivera, W. B. Daniel, S. Y. Chen, and R. E. Ecke, Phys. Rev. Lett. **90**, 104502 (2003).

[19] Y. Amarouchene, D. Bonn, J. Meunier, and H. Kellay, Phys. Rev. Lett. **86**, 3558 (2001).